

# Lipopolysaccharide-induced splenic ferroptosis in goslings was alleviated by polysaccharide of *Atractylodes macrocephala koidz* associated with proinflammatory factors

Wanyan Li,<sup>\*,†,1</sup> Xiangying Zhou<sup>OR,\*,†,1</sup> Shiwen Xu,<sup>‡</sup> Nan Cao,<sup>\*,†</sup> Bingxin Li,<sup>\*,†</sup> Wenbin Chen,<sup>\*,†</sup> Baohe Yang,<sup>§</sup> Mingfeng Yuan,<sup>§</sup> and Danning Xu<sup>\*,†,2</sup>

<sup>\*</sup>College of Animal Science & Technology, Zhongkai University of Agriculture and Engineering, Guangzhou 510225, China; <sup>†</sup>Guangdong Province Key Laboratory of Waterfowl Healthy Breeding, Guangzhou 510225, China; <sup>‡</sup>College of Veterinary Medicine, Northeast Agricultural University, Harbin 150030, China; and <sup>§</sup>Yunnan Kuaidaduo Animal Husbandry Technology Co., Ltd, Yuxi 653100, China

**ABSTRACT** Ferroptosis is a newly discovered form of cell death due to iron-dependent lipid peroxidation. In animal breeding, many environmental factors could lead to oxidative stress, which in turn reduce animal immunity and production performance. Polysaccharide of *Atractylodes macrocephala* Koidz (**PAMK**) has antioxidant, immunomodulatory, and inflammatory modulating effects. For investigating the effect of PAMK on splenic ferroptosis in gosling caused by lipopolysaccharide (**LPS**), 40 one-day-old Magang goslings were randomly divided into 4 groups (CON group, LPS group, PAMK group, and LPS+PAMK group). The protein expression of the ferroptosis marker Glutathione Peroxidase 4 (**GPX4**), the relative mRNA expression of ferroptosis-related genes and cytokines, and the oxidative stress and iron content of spleen tissues were examined. The correlation between ferroptosis and inflammatory factors was further analyzed by principal component

analysis. The results showed that, compared with CON group, LPS caused alterations in the expression of the ferroptosis pathway genes and cytokines, which could upregulate levels of ferroptosis and inflammation. However, after treated with PAMK, the inflammation and ferroptosis was alleviated. Meanwhile, PAMK restored the expression and distribution of GPX4. In addition, PAMK alleviated the oxidative stress caused by LPS and reduced the iron content in spleen. Principal component analysis showed that cytokines were more closely related to antioxidant indexes. The CON, PAMK and LPS+PAMK groups had similar effects on the four components, with the LPS and PAMK groups showing the furthest difference in results. The result indicated that PAMK could reduce the level of oxidative stress and inflammatory cytokines in spleen of gosling caused by LPS, and jointly alleviate ferroptosis by regulating genes related to the ferroptosis pathway.

**Key words:** polysaccharide of *Atractylodes macrocephala* Koidz (PAMK), lipopolysaccharide (LPS), ferroptosis, principal component analysis, antioxidant index

2022 Poultry Science 101:101725

<https://doi.org/10.1016/j.psj.2022.101725>

## INTRODUCTION

Ferroptosis, a new mode of programmed cell death discovered in recent years, is caused by iron-dependent lipid peroxidation-induced oxidative damage to cells (Dixon et al., 2012). Many studies have shown that the occurrence of ferroptosis mainly involves iron transport, downregulation of cystine/glutamate antiporter system

activity, glutathione depletion, and accumulation of reactive oxygen species (**ROS**) (Xie et al., 2016). The molecular mechanisms involved in ferroptosis are broad, as it can be stimulated by a variety of different compounds and regulated by multiple forms of upstream signaling pathways, but ultimately all are induced through an increase in ROS. In the presence of lipoxygenases (**LOX**) or Fe<sup>2+</sup>, polyunsaturated fatty acids on cell membranes are catalyzed, causing lipid peroxidation, leading to a continuous accumulation of ROS and attacking the biofilm, which eventually triggers ferroptosis (Cheng and Li, 2007). Ferroptosis leads to metabolic dysfunction and massive lipid peroxidation, which imbalances intracellular lipid peroxide production and degradation and ultimately causes oxidative stress. It

© 2022 The Authors. Published by Elsevier Inc. on behalf of Poultry Science Association Inc. This is an open access article under the CC BY-NC-ND license (<http://creativecommons.org/licenses/by-nc-nd/4.0/>).

Received November 10, 2021.

Accepted January 8, 2022.

<sup>1</sup>These authors contributed equally.

<sup>2</sup>Corresponding author: [xdanning212@126.com](mailto:xdanning212@126.com)

has been shown that oxidative stress damages the spleen lymphocytes of chickens and reduces the immunity of the organism (Bi et al., 2019). Oxidative stress disrupts the balance of oxidative and antioxidant systems in the body, decreasing the productive performance and immunity of animals and even inducing diseases. Ferroptosis has also been reported to play an important role in several inflammatory diseases and conditions (Yang et al., 2014; Li et al., 2019c).

During the breeding of animals, many environmental factors can lead to oxidative stress in the animal organism, including lipopolysaccharide (LPS). As a major component of gram-negative bacterial outer membrane toxicity, LPS activates mononuclear macrophages and causes a large release of inflammatory cytokines, leading to the development of inflammation and causing apoptosis, necrosis and pyroptosis of normal cells (Farghali et al., 2015; Li et al., 2019a). In addition, LPS promotes the production of ROS (Chen et al., 2017). When too many free radicals are produced in animals and cannot be scavenged in time, they can cause oxidative stress (Reuter et al., 2010). The animal breeding environment is prone to the growth of harmful bacteria, leading to an increase in the concentration of LPS in animals, which brings adverse effects on the growth and development of animals and production efficiency.

It has been reported that ferroptosis in cells could be caused by LPS, and Cyclooxygenase 2 (COX-2) is a recognized marker of ferroptosis (Karuppagounder et al., 2018). Ferroptosis could be caused by ROS, and the increasing level of ROS is also important for the occurrence of ferroptosis (Xie et al., 2016). Li found that inhibition of ferroptosis alleviated the increasing ROS in the heart of mice induced by LPS (Li et al., 2020). In LPS-induced rheumatoid arthritis, LPS is involved in the regulation of the cystine/glutamate antiporter system/GPX4 axis as well as lipid ROS levels (Luo and Zhang, 2021). In addition, ferroptosis is involved in LPS-induced acute lung injury (Liu et al., 2020). Meanwhile, lots of evidence prove that ferroptosis is also involved in the regulation of various diseases associated with inflammatory responses (Kain et al., 2019; Proneth and Conrad, 2019). However, the involvement of ferroptosis in the regulation of the LPS-induced splenic oxidative stress in a model of goslings has not been reported.

Polysaccharide of *Atractylodes macrocephala* Koidz (PAMK) is a major active ingredient extracted from the traditional Chinese medicine *Atractylodes macrocephala* with growth-promoting, antioxidant, antibacterial, immunity enhancement, and antitumor effects (Wang et al., 2013; Li et al., 2014; Shu et al., 2017). Our previous studies also found that PAMK not only could alleviate LPS-induced tissue inflammatory damage (Guo et al., 2021; Li et al., 2021b), but also could improve immunosuppression induced by cyclophosphamide (Li et al., 2018; Xiang et al., 2020; Li et al., 2021a). At the same time, PAMK could regulate splenic lymphocyte immune function in chicken through activating TLR4/NF- $\kappa$ B signaling pathway (Li et al., 2019b). In

addition, PAMK could also alleviate immune dysfunction in spleen of chicken induced by heat stress via reducing oxidative stress, enhancing mitochondrial function, and inhibiting apoptosis (Xu et al., 2017).

Based on the researches above, we speculate that PAMK can alleviate ferroptosis in the spleen of goslings caused by LPS. To verify this hypothesis, we constructed a splenic oxidative stress model with LPS, and then detected ferroptosis-related indicators, the expression of cytokines and GPX4. Therefore, in this study, we want to explore the mechanism that PAMK alleviate ferroptosis in spleen of gosling caused by LPS and provide the theoretical basis for the development of PAMK as a green feed additive that can replace antibiotics for the healthy breeding of animals.

## MATERIALS AND METHODS

### *Animal Experimental Design*

All goslings were purchased from Guangdong Qingyuan Jinyufeng Goose Co., Ltd., China. Forty 1-day-old Magang goslings (half male and half female) were randomly divided into 4 groups of 10 goslings each and pre-fed for 3 d. The goslings in the PAMK and LPS +PAMK groups were fed a diet containing 400 mg/kg PAMK (Purity 95%, Yanglingciyuan Biotechnology Company, Xi'an, China); the CON group and LPS group were fed a normal diet. The goslings in the LPS and LPS+PAMK groups were injected intraperitoneally with 2 mg/kg · BW of LPS (L2880, Sigma, Saint Louis, MO) in a volume of 1 mL at the same time at 24, 26, and 28 ds of age; the CON and PAMK groups were injected with a phase of 1 mL saline at the same time. The goslings in all four groups were allowed to free access to feed and water, fed in free-range and were given equal amounts of green vegetables. At 28 d of age, spleen tissue was collected one hour after the injection of LPS. Ten samples were collected in each group and part of them was frozen at  $-80^{\circ}\text{C}$  and the other part was fixed with 4% paraformaldehyde and used for immunohistochemistry. And ethical approval for this experiment was obtained from Zhongkai University of Agriculture and Engineering with the approved protocol NO. 20200101.

### *Real-Time Quantitative PCR*

Total RNA was extracted from spleen of goslings using TRIzol reagent according to the manufacturer's reagent instructions (15596026, Ambion, Austin, TX). The extracted total RNA was reverse transcribed using reverse transcription reagent (RR036A, Takara, China), and the resulting cDNA was stored at  $-20^{\circ}\text{C}$ . Primer sequences were designed according to the NCBI database (Table 1). The ABI PRISM 7500 detection system (Applied Biosystems, Foster city, CA) was used to detect the relative mRNA expression of the genes. In this assay,  $\beta$ -actin was used as an internal reference gene, and the mRNA expression of each gene was

**Table 1.** Primer sequences for qPCR.

Gene	Primer (5' → 3')	
$\beta$ -actin-F	GCACCCAGCACGATGAAAAAT	XM_013174886.1
$\beta$ -actin-R	GACAAATGGAGGGTCCGGATT	
GPX4-F	TCGATGTGAAATGGGGACGAC	XM_013200057.1
GPX4-R	GTCCTTCTCGATGACGTAGGG	
ACSL4-F	GCGGCTGAAACCCCTTCTT	XM_013185083.1
ACSL4-R	GCCAACAGTGGACACAAGCTA	
NOX1-F	CGGAGATGCCCGGATTGA	XM_013183388.1
NOX1-R	CGGCAGAGCCAGTAGAAGTAG	
TFR1-F	AGAATGGCTGGAGGGGTACT	XM_013195023.1
TFR1-R	TTCTCTCCAGCAGCCATAC	
FTH1-F	ATGGTCATGGCCTTTCCCC	XM_013177583.1
FTH1-R	AATGAAGTCACACAGATGCGG	
FPN1-F	CTGGGGAGATCGTATGTGGC	XM_013178636.1
FPN1-R	AGGATGTCTGGGCCACTTTG	
HSPB1-F	CTCCGAGATCCGCCAAAG	XM_013189820.1
HSPB1-R	GAAGCCGTGCTCATCCTGT	
COX-2-F	TGTCCTTTCCTACTGCTTTCCAT	XM_013177944.1
COX-2-R	TTCCATTGCTGTGTTTGAGGT	
IFN- $\gamma$ -F	CCAGATTGTTTCCCTGTACTTG	XM_013198313.1
IFN- $\gamma$ -R	CATCAGAAAAGGTTGTCTCTCA	
IL-1 $\beta$ -F	AAGTGAGGCTCAACATTGCG	XM_015297469.2
IL-1 $\beta$ -R	CGGTAGAAGATGAAGCGGGT	
IL-4-F	GGCATCTACCTCAACTTGCT	XM_013175717.1
IL-4-R	CTCTTTTCGCTACTCGTTGGA	
IL-6-F	ACGATAAGGCAGATGGTGAT	XM_013171777.1
IL-6-R	TCCAGGTCTTATCCGACTTC	
IL-10-F	ATCATGACATGGACCCGTA	XM_013189578.1
IL-10-R	ATTGCTCCATGACAGTTGCT	
IL-17-F	CATGTTGTCAGGCCAGATTCT	NM_204460.2
IL-17-R	CATCTTTTTGGGTTAGGCATCC	
IL-18-F	GCCTTACTTTGCTGACGATG	XM_013187166.1
IL-18-R	ACCACAAGCACCTGGCTATTT	
TNF- $\alpha$ -F	GTTCTATGACCGCCAGTTC	XM_013189516.1
TNF- $\alpha$ -R	CACACGACAGCCAAGTCAA	

calculated using the  $2^{-\Delta\Delta ct}$  relative quantification method and normalized to the expression relative to the CON group.

### ROS level, T-AOC, GSH, MDA, and Iron Content Assays

The ROS (XY-ELA08632) level assay was performed using the kit (Shanghai Xinyu Biotechnology Company, Shanghai, China) according to the manufacturer's instructions, and the T-AOC (A015-2-1), GSH (A006-2-1), MDA (A003-1-2), and tissue iron (A039-2-1) content assay were performed using the kit (Nanjing Jiancheng Institute of Biological Engineering, Nanjing, China) according to the manufacturer's instructions.

### Immunohistochemistry

Spleen sections were dewaxed in xylene and hydrated with a gradient ethanol solution. Antigen repair was performed on the sections using EDTA antigen repair buffer (G5012, Servicebio, Wuhan, China). Endogenous peroxidase was blocked with 3% hydrogen peroxide solution. The tissue was uniformly covered with 3% BSA (A8020, Solarbio, Beijing, China) and closed at room temperature for 30 min. GPX4 primary antibody (1:1,000, ab40993, Abcam, Cambridge, UK) was added, incubated overnight at 4°C and washed with PBS.

Added secondary antibody (1:200, G1215, Servicebio), incubated for 50 min at room temperature, and washed with PBS. DAB color development solution (G1215, Servicebio) was added, and the color development time was controlled under the microscope (Nikon, Tokyo, Japan). The sections were rinsed with water to terminate the color development. Harris hematoxylin (G1004, Servicebio) was used to stain the cell nucleus for 3 min, 1% hydrochloric acid was used for differentiation, and ammonia was used to return the blue. The sections were dehydrated and dried by gradient alcohol, transparent in xylene, sealed with neutral gum, dried, and examined microscopically. Used Image J to calculate the IOD, the ratio of IOD to the total area of the image is the mean density.

### Statistical Analysis

The experimental data were analyzed by one-way ANOVA using GraphPad Prism 7.0. The differences between 4 groups were compared by Tukey's multiple comparison method, and the results were expressed as "mean  $\pm$  SEM", with  $P < 0.05$  being considered significant. In addition, the data of the 21 indicators obtained from the trial were standardized to make the data conform to normal distribution and comparable. The data were analyzed by principal component analysis using SPSS Statistics 26 to analyze the relationship between the indicators.

## RESULTS

### PAMK Alleviated LPS-Induced Disruption of Relative mRNA Expression of Splenic Ferroptosis Pathway Gene

The relative mRNA expression of ferroptosis pathway genes was examined by RT-PCR in the spleen of goslings (Figure 1). Among the genes related to the inhibition of ferroptosis, the mRNA expression of *GPX4*, *FTH1*, and *FPN1* was significantly ( $P < 0.05$ ) lower in the LPS group compared with the CON group, except for *HSPB1*. The stimulation of LPS significantly increased the mRNA expression of *COX-2*, *NOX1*, *TFR1* and *ACSL4* ( $P < 0.05$ ), which are genes related to the promotion of ferroptosis. In contrast, the mRNA expression of *GPX4*, *FTH1*, *COX-2*, *NOX1*, and *ACSL4* were not differentially significant in the LPS+PAMK group compared with the CON group. Among them, the expression of mRNAs of *FPN1*, and *TFR1* in the LPS +PAMK group did not return to the same level as the CON group, but had a similar trend development as the CON group, and the difference was significant compared with the LPS group ( $P < 0.05$ ). The above results showed that LPS stimulation caused changes in the expression of *GPX4*, *FTH1*, and other genes of the ferroptosis pathway, resulting in elevated levels of ferroptosis, which was alleviated by PAMK treatment.

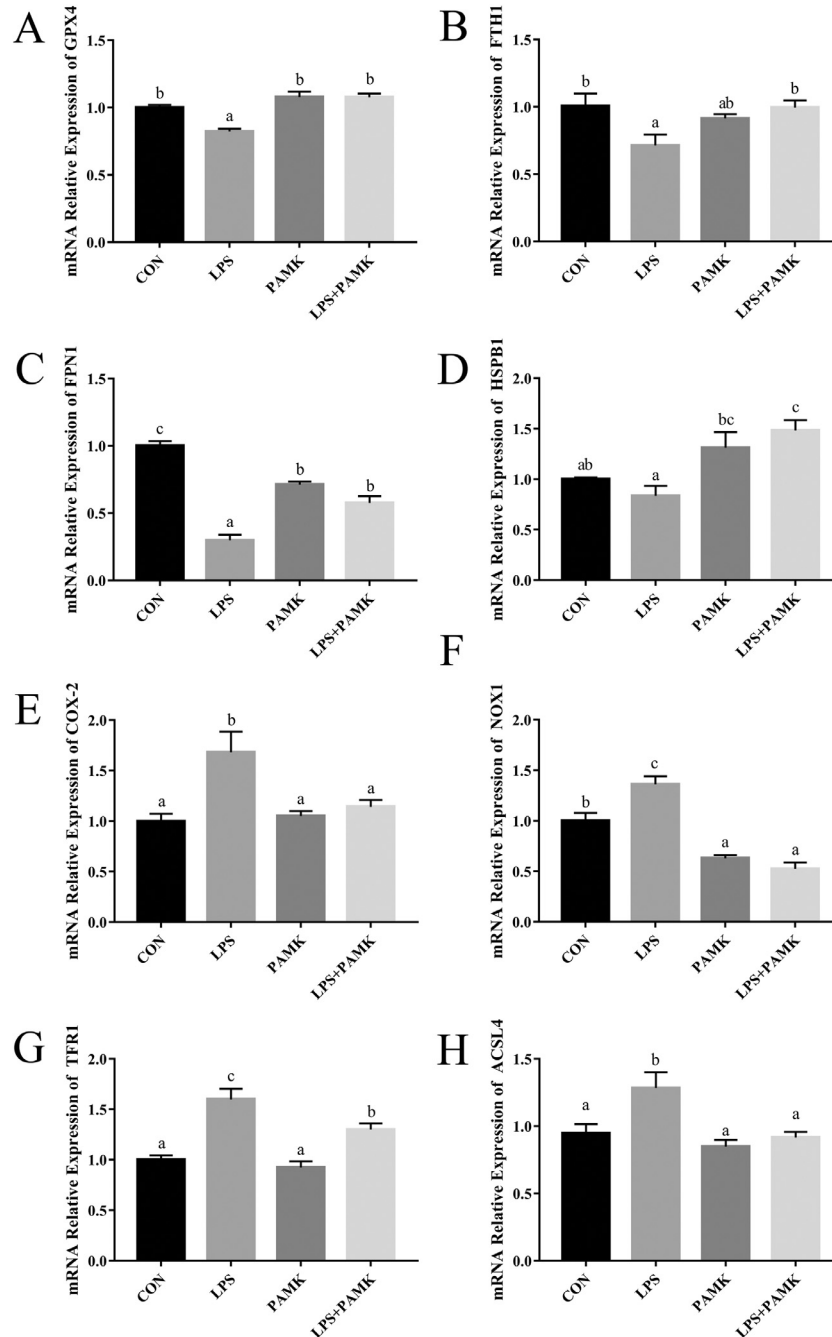


**Figure 1.** Effects of PAMK on the relative mRNA expression of splenic ferroptosis pathway gene treated with LPS. Relative mRNA expression of (A) GPX4; (B) FTH1; (C) FPN1; (D) HSPB1; (E) COX-2; (F) NOX1; (G) TFR1; (H) ACSL4. Data are expressed as the means  $\pm$  SEM,  $n = 10$ . Different letters indicate  $P < 0.05$ , significantly different. Abbreviations: LPS, lipopolysaccharide; PAMK, polysaccharide of *Atractylodes macrocephala* Koidz.

### **PAMK Alleviated LPS-Induced Elevated Levels of Oxidative Stress in Spleen**

The antioxidant indexes of the spleen of the goslings were examined (Figure 2). Compared to the CON group, both GSH content and T-AOC were significantly decreased in the LPS group ( $P < 0.05$ ), and the concentration of MDA was significantly increased ( $P < 0.05$ ). Compared with the LPS group, the T-AOC was significantly increased ( $P < 0.05$ ) and the concentration of MDA was significantly decreased ( $P < 0.05$ ) in the LPS+PAMK group. As for the content of GSH and the levels of ROS, although there was no significant difference in the LPS

+PAMK group compared with the LPS group ( $P > 0.05$ ), had the opposite trend to the LPS group. This suggested that the level of oxidative stress in the spleen of goslings was increased under the stimulation of LPS, and PAMK could alleviate this phenomenon.

### **PAMK Alleviated LPS-Induced Increase in Iron Content in Spleen**

The iron content of the spleen tissues of the goslings was examined (Figure 2E). Compared with the CON group, the iron content of spleen tissues in the LPS



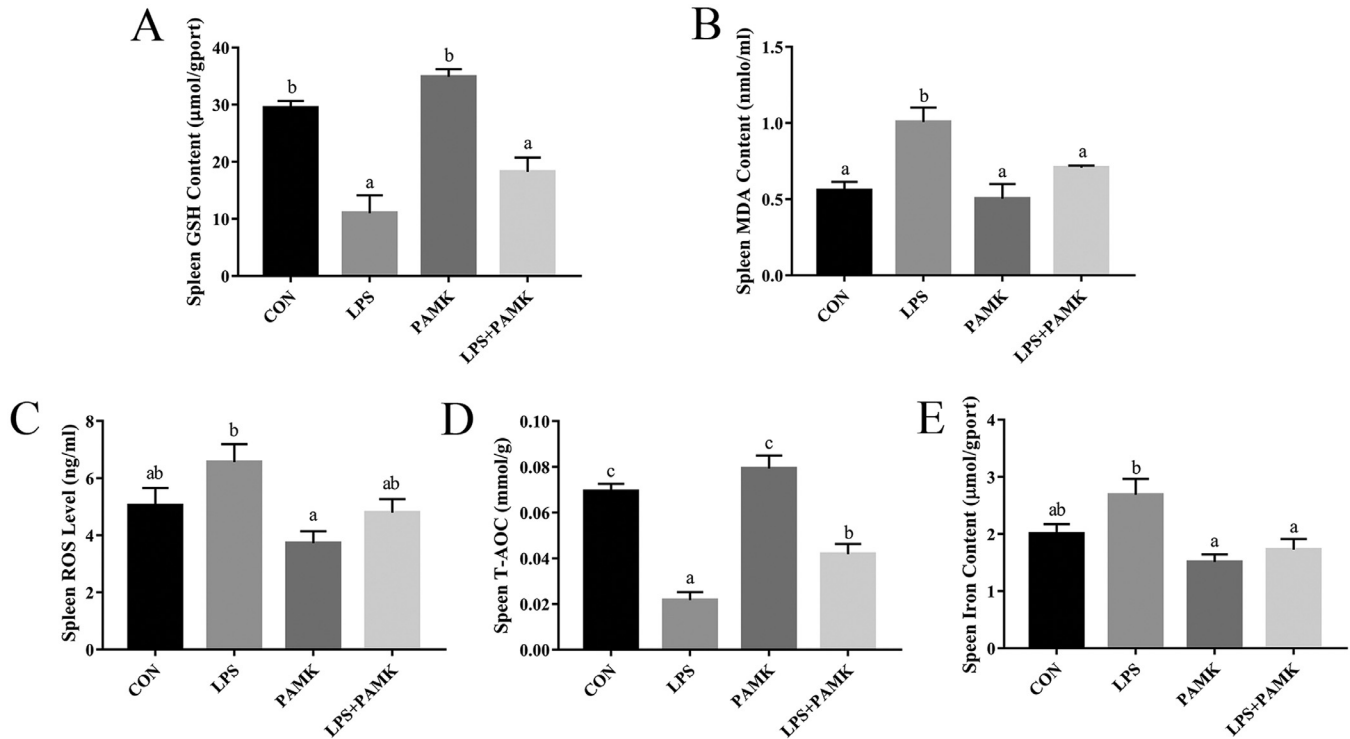


**Figure 2.** Effects of PAMK on levels of oxidative stress and iron content in spleen treated with LPS. (A) GSH content; (B) MDA content; (C) ROS level; (D) T-AOC; (E) Iron content. Data are expressed as the means  $\pm$  SEM,  $n = 10$ . Different letters indicate  $P < 0.05$ , significantly different. Abbreviations: LPS, lipopolysaccharide; PAMK, polysaccharide of *Atractylodes macrocephala* Koidz.

group showed an increasing trend, although there was no significant difference ( $P > 0.05$ ). And the iron content of the LPS+PAMK group was significantly lower ( $P < 0.05$ ) compared with the LPS group. The results indicated that PAMK could significantly down-regulate the LPS-induced increase of iron content in the spleen of goslings.

### **PAMK Alleviated LPS-Induced Ferroptosis in Spleen**

Protein expression of GPX4 in spleen tissue detected by immunohistochemistry (Figure 3). The results showed that the protein level of GPX4 in the spleen was significantly downregulated after intraperitoneal injection of LPS ( $P < 0.05$ ). In addition, there was no significant difference in the protein levels of GPX4 in the spleens of the CON, PAMK, and LPS+PAMK groups. This indicates that stimulation by LPS leads to a significant decrease in the protein level of GPX4 in the spleen of goslings. This leads to a weakening of the role of GPX4 in catalyzing lipid peroxide substrates, resulting in a decrease in cellular antioxidant capacity, a buildup of lipid ROS, and ultimately ferroptosis.

### **PAMK Alleviates the Increase in Relative mRNA Expression of Splenic Cytokine Induced by LPS**

The spleens of goslings were examined for the relative expression of cytokine mRNA by RT-PCR (Figure 4).

LPS group significantly increased the mRNA expression of *IFN- $\gamma$* , *IL-1 $\beta$* , *IL-4*, *IL-6*, *IL-10*, and *IL-17* in the spleen of goslings compared with the CON group ( $P < 0.05$ ), but there was no significant difference in the mRNA expression of *IL-18* and *TNF- $\alpha$* . In addition, here was no significant difference in the expression of mRNA of the above cytokines in the PAMK group compared to the CON group, except for *IL-18*. However, the results of the LPS+PAMK group revealed a significant decrease in mRNA expression of cytokines except *IL-4*, *IL-6*, and *TNF- $\alpha$*  compared from the results of the LPS group ( $P < 0.05$ ) and were closer to the CON group. Interestingly, the *IL-4* level in the LPS+PAMK group was instead significantly higher compared with the LPS group ( $P < 0.05$ ). The *TNF- $\alpha$*  level in the LPS group was not significantly different from those in the CON group, but there was a tendency to increase. And the expression of *TNF- $\alpha$*  after co-treatment with LPS and PAMK was more similar to that of the CON group. In other words, LPS stimulated an increase in splenic tissue inflammatory cytokines in goslings, whereas PAMK downregulated the increase in splenic inflammatory cytokine levels caused by LPS.

### **Principal Component Analysis**

The parameters obtained in this study were subjected to principal component analysis and 4 principal components were extracted, each with eigenvalues greater than 1, and the total percentage of variance of the 4 principal components was 81.184%. Therefore, the four

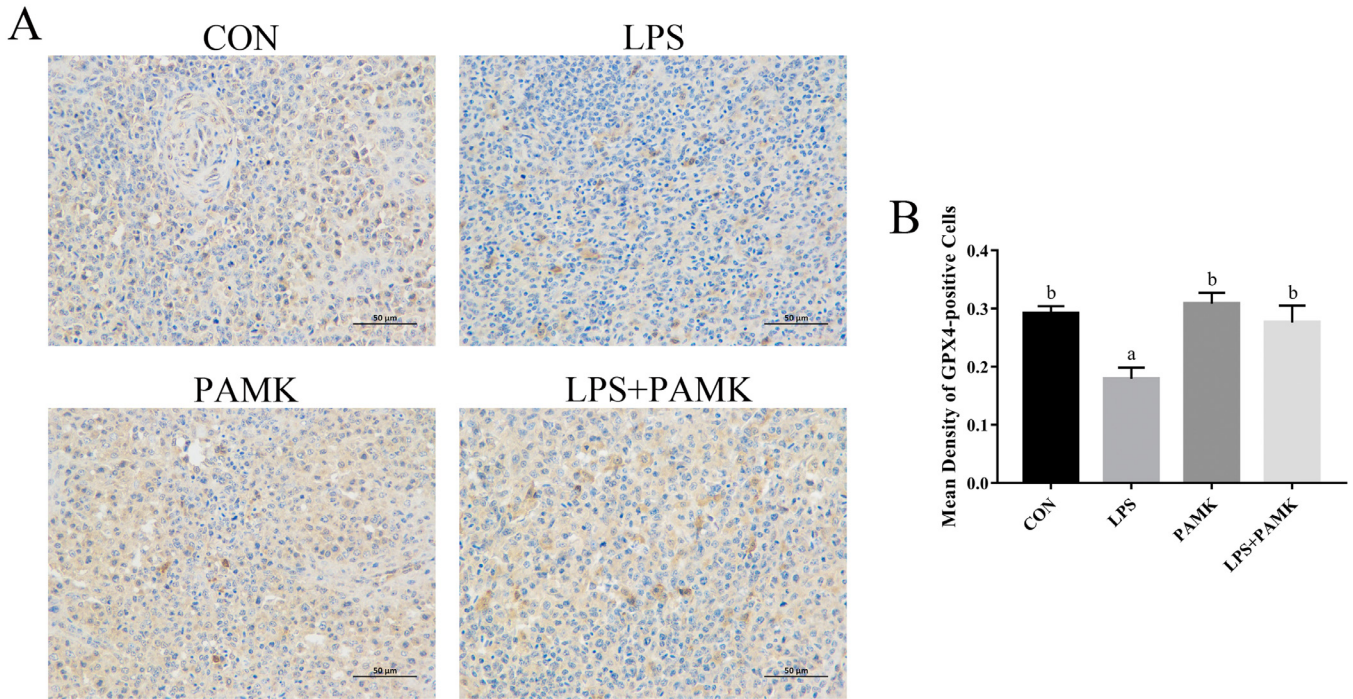


**Figure 3.** (A) Effects of PAMK on protein expression of GPX4 in spleen treated with LPS, bars 50  $\mu\text{m}$ . (B) Mean density of GPX4-positive cells. Data are expressed as the means  $\pm$  SEM. Different letters indicate  $P < 0.05$ , significantly different. Abbreviations: LPS, lipopolysaccharide; PAMK, polysaccharide of *Atractylodes macrocephala* Koidz.

principal components can represent most of the variance of the results (Table 2).

In the rotated component matrix (Table 3), the first principal component had greater positive correlations with *IL-4*, *IL-10*, *IL-17*, and MDA, and greater negative correlations with *FPN1*. Of interest, the second principal component had a greater positive correlation with *TFR1*, iron, ROS, *IFN- $\gamma$* , and *TNF- $\alpha$* . The major positive correlation with the third principal component was *NOX1*, whereas the major negative correlations were *GPX4* and *HSPB1*.

The scores of each of the 4 components were used to calculate the scores of the different groups on each principal component (Table 4). The results showed that the CON and LPS groups had a greater effect on the first principal component and that these 2 groups had an opposite effect on it. It is noteworthy that the LPS group had the largest effect on the second principal component. Also, the scores of the CON group, the PAMK group, and the LPS+PAMK group were relatively close in the 4 components, indicating that the effects of these 3 groups on the 4 components were similar. In contrast, the scores of the LPS group were more different from the other 3 groups, indicating that the effect of the LPS group on the 4 components was very different from the other 3 groups.

Based on the scores of the different indicators on the 3 components (Table 3), a three-dimensional component map was constructed (Figure 5). The three-dimensional component map showed that all indicators were divided into 2 main clusters. Comparison of the 2 major clusters reveals that the indicators promoting ferroptosis (*NOX1*, *TFR1*, *COX-2*, *ACSL4*, ROS, iron, and MDA)

and most of the cytokines (*IL-1 $\beta$* , *IL-4*, *IL-6*, *IL-10*, *IL-17*, *IL-18*, and *IFN- $\gamma$* ) are mainly clustered in the upper left corner, and the indicators inhibiting ferroptosis (*GPX4*, *FPN1*, *FTH1*, GSH, and T-AOC) were mainly clustered in the lower right corner.

## DISCUSSION

The occurrence of cellular ferroptosis mainly involves the accumulation of lipid peroxides, and the production of lipid peroxides depends on the intracellular iron Fenton reaction, and its clearance is mainly accomplished by Glutathione Peroxidase 4 (GPX4). Therefore, iron, lipid peroxides and GPX4 can be considered as 3 key factors of ferroptosis. It was found that the expression of ferroptosis-related factors in jejunal epithelial cells of weaned piglets was changed and the antioxidant capacity was reduced under the stimulation of LPS, indicating that LPS could promote ferroptosis in jejunal epithelial cells of piglets (Hua et al., 2019). HSPB1, TFR1, FTH1 and FPN1 are all key proteins involved in intracellular iron metabolism (Zhang et al., 2011; Gao et al., 2015; Hou et al., 2016). In this study, the results showed that PAMK could rescue LPS-induced ferroptosis by increasing the expression of genes related to iron storage (ferritin heavy chain, *FTH1*) and iron export (ferritin transport, *FPN1*) and by decreasing the expression of the membrane protein transferrin receptor 1 (*TFR1*), which is associated with the transfer of iron ions into cells. It has been reported that *COX-2* expression is regulated by *ACSL4* and upregulation of the *ACSL4*-*COX2* pathway is important for the occurrence of

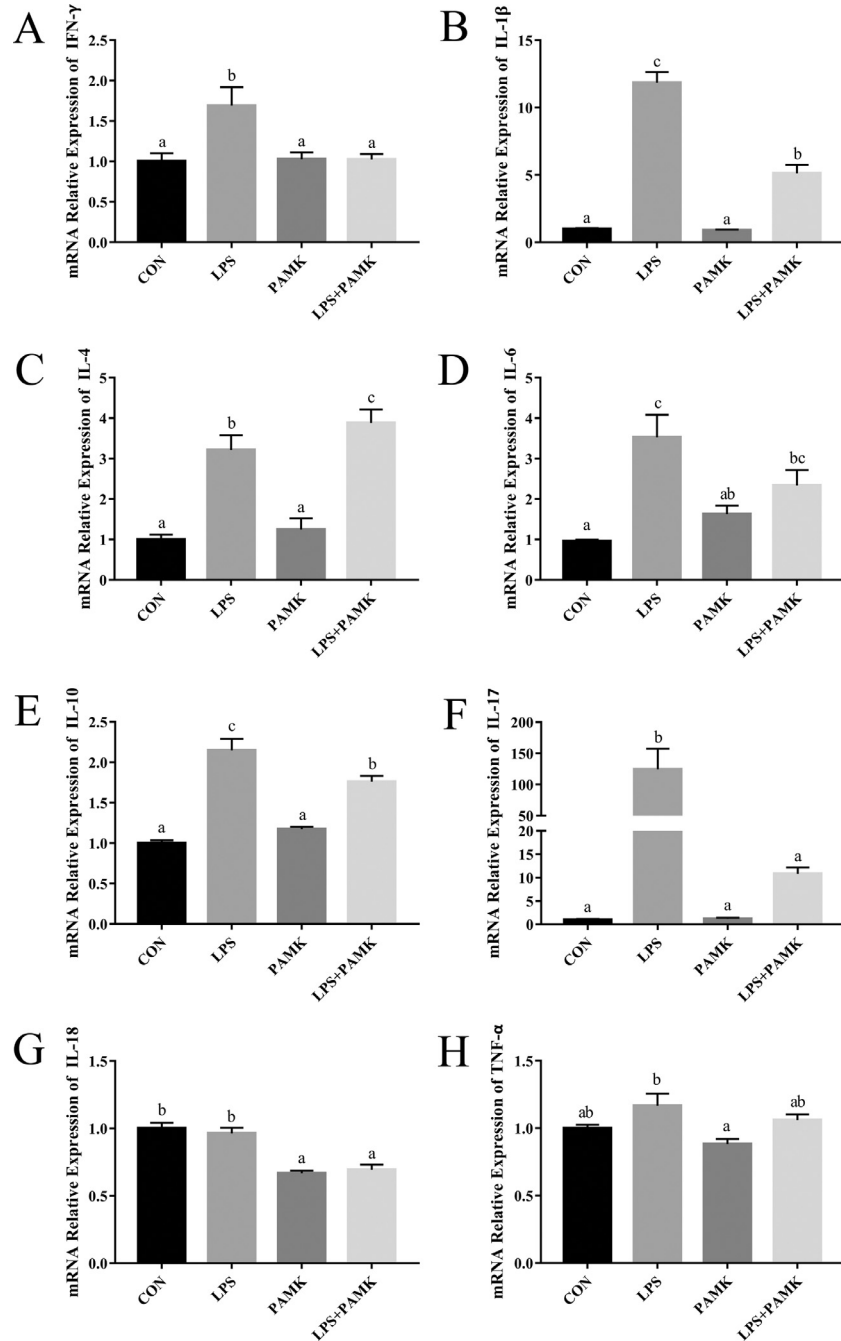


**Figure 4.** Effects of PAMK on the relative mRNA expression of Splenic Cytokine treated with LPS. Relative mRNA expression of (A) IFN- $\gamma$ ; (B) IL-1 $\beta$ ; (C) IL-4; (D) IL-6; (E) IL-10; (F) IL-17; (G) IL-18; (H) TNF- $\alpha$ . Data are expressed as the means  $\pm$  SEM, n = 10. Different letters indicate  $P < 0.05$ , significantly different. Abbreviations: LPS, lipopolysaccharide; PAMK, polysaccharide of *Atractylodes macrocephala* Koidz.

ferroptosis (Maloberti et al., 2010). PAMK can reduce the increase in the expression of *NOX1* (an important catalase for ROS production), *COX-2* (involved in inflammatory response and ferroptosis process), and *ACSL4* caused by LPS. The results suggested that

**Table 2.** Principal components and extracted sums of variance measures in goslings.

Component	Total	% of Variance	Cumulative %
1	9.803	46.681	46.681
2	3.386	16.122	62.803
3	2.505	11.931	74.734
4	1.354	6.450	81.184

PAMK might affect ferroptosis in spleens by regulating the expression of key genes.

It has been shown that T cell death induced by GPX4 deficiency is caused by a lipid peroxide-mediated pathway involving ferroptosis (Matsushita et al., 2015). GPX4 can reduce intracellular ROS by using GSH as an electron donor (Yang et al., 2014). Membrane polyunsaturated lipids are susceptible to oxidation by excess ROS in the cytoplasm, leading to the production of end products such as MDA, which reduces the antioxidant capacity of the organism and causes ferroptosis (Mishima et al., 2020). Accumulation of ROS and down-regulation of GPX4 expression have been found to occur in LPS-induced acute lung injury (Liu et al., 2020). To

**Table 3.** The rotated component matrix.

Indicators	Component 1	Component 2	Component 3	Component 4
Relative mRNA expression of GPX4	-0.148	-0.504	-0.677	-0.260
Relative mRNA expression of ACSL4	-0.115	-0.019	0.111	-0.066
Relative mRNA expression of NOX1	0.399	0.426	0.782	0.046
Relative mRNA expression of TFR1	0.300	0.863	0.008	0.074
Relative mRNA expression of FTH1	-0.625	-0.040	-0.337	-0.438
Relative mRNA expression of FPN1	-0.736	-0.204	-0.396	-0.327
Relative mRNA expression of HSPB1	0.035	0.121	-0.929	-0.135
Relative mRNA expression of COX2	0.199	-0.178	0.144	0.905
Relative mRNA expression of IFN- $\gamma$	0.152	0.875	0.148	-0.127
Relative mRNA expression of IL-1 $\beta$	0.470	0.505	0.350	0.618
Relative mRNA expression of IL4	0.846	0.079	-0.159	0.294
Relative mRNA expression of IL6	0.683	-0.202	0.173	0.516
Relative mRNA expression of IL10	0.893	0.253	0.058	0.191
Relative mRNA expression of IL17	0.806	0.233	0.415	-0.250
Relative mRNA expression of IL18	0.219	0.039	0.621	0.145
Relative mRNA expression of TNF- $\alpha$	0.026	0.775	-0.262	-0.324
Spleen ROS level	0.083	0.690	0.288	0.404
Spleen MDA concentration	0.831	0.417	0.161	0.002
Spleen GSH content	-0.643	-0.448	-0.035	-0.566
Spleen T-AOC	-0.626	-0.637	0.077	-0.198
Spleen Iron content	0.206	0.810	0.395	-0.016

**Table 4.** Scores of the four groups of goslings on four principal components.

Group	Component 1	Component 2	Component 3	Component 4	Total	Ranking
CON	-0.883	-0.214	0.580	-0.422	-0.938	3
LPS	0.860	0.942	0.704	0.692	3.197	1
PAMK	-0.513	-0.334	0.047	-0.321	-1.121	4
LPS+PAMK	0.461	-0.004	-1.164	0.325	-0.382	2

further verify the involvement of LPS in the induction of ferroptosis in the spleen of goslings and the role of PAMK, we examined the expression of GPX4 protein in spleen by immunohistochemistry. The results showed that LPS significantly reduced the protein level of GPX4, indicating the involvement of LPS in stimulating ferroptosis in the spleen. In contrast, co-treatment of PAMK and LPS restored the protein expression of GPX4 to the level of the CON group, indicating that PAMK could effectively alleviate the LPS-involved ferroptosis in spleen. Our study showed that LPS treatment leads to excessive accumulation of ROS and MDA, resulting in depletion of GSH, reduction of GPX4, enhancing lipid peroxidation and decreasing total antioxidant capacity. This peroxidation was alleviated after the addition of PAMK. It is suggested that PAMK scavenges lipid peroxidation ROS and MDA by increasing the expression of GPX4, while increasing the content of its cofactor GSH, thus improving the antioxidant capacity of the body and alleviating ferroptosis.

Iron is essential for animal survival, and host cells can also use iron to produce ROS to scavenge microbes and promote cell survival (Grenier et al., 2001). However, excessive free iron accumulation in the cytoplasm may promote excessive accumulation of ROS and lead to cellular ferroptosis (Zhao et al., 2020). Inflammatory mediators such as IL-6 and LPS can directly trigger the production of hepcidin, leading to the accumulation of intracellular iron and a decrease in circulating iron levels (Nemeth et al., 2004; Armitage et al., 2011). In the case of microbial infection, immune cells release several

inflammatory factors, among which IL-1, IL-6, and IL-22 have specific effects on iron metabolism (Nicolas, 2002; Kemna et al., 2005; Muckenthaler et al., 2017). Our results showed that PAMK could alleviate the LPS-induced elevation of iron levels in spleen of goslings. This suggests that PAMK can alleviate ferroptosis by regulating iron levels in tissues, which may not only regulate key genes involved in intracellular iron metabolism, but also affect cytokine transcription.

As the largest peripheral immune organ of the body, the spleen contains a large number of lymphocytes and macrophages and is the center of cellular and humoral immunity of the body. Cytokine production is important for the body to maintain autoimmunity, but too much cytokine can be harmful to the body. LPS can cause the release of inflammatory mediators in the body, leading to cytokine storm and even tissue inflammation and cell death. Xiao et al. (2015) found that intraperitoneal injection of LPS in rats was able to cause acute damage or severe infection of spleen. ROS is the main cause of the expression of proinflammatory factors IL-1 $\beta$ , TNF- $\alpha$ , and the proinflammatory enzyme COX-2 (Qiang et al., 2014). In addition, iron status has been shown to alter cytokine levels and iron homeostasis is a potential target for the regulation of inflammation (Xiong et al., 2003; Wang et al., 2009; Kroner et al., 2014). Previous studies by our group demonstrated that PAMK could regulate LPS-mediated hepatitis in mice through the TLR4-MyD88-NF $\kappa$ B signaling pathway, decreasing IL-1 $\beta$ , IL-6, and TNF- $\alpha$  levels and elevating IL-4 levels (Guo et al., 2021). Therefore, for a more



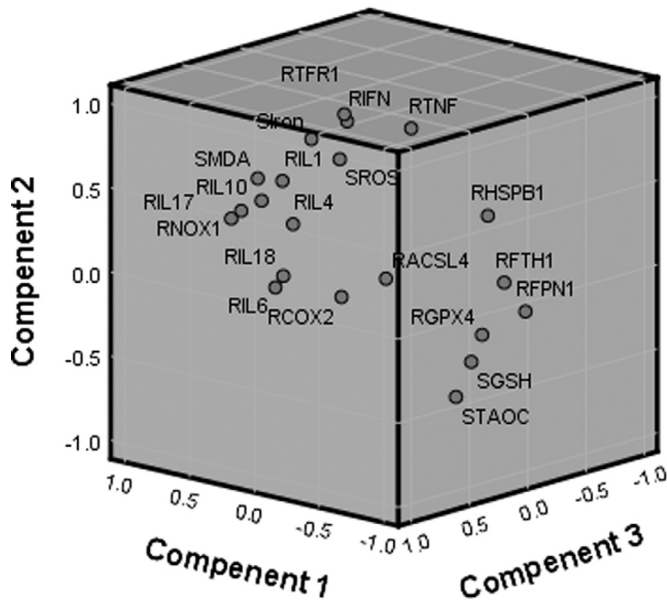


**Figure 5.** The component plot of the principal component analysis in goslings.

comprehensive understanding of the mechanism of action of PAMK in alleviating ferroptosis in spleen of goslings, we examined the expression of cytokines. Our results also showed that the expression of pro-inflammatory cytokines *IFN- $\gamma$* , *IL-1 $\beta$* , *IL-6*, *IL-10*, and *IL-17* upregulated under the stimulation of LPS. In contrast, the mRNA expression of other cytokines, except *IL-4*, *IL-6*, and *TNF- $\alpha$* , significantly reduced after the addition of PAMK. Ludwiczek found that inflammatory cytokines such as TNF, *IFN- $\gamma$* , and *IL-10* stimulate the transcription of TFR1 (Ludwiczek et al., 2003). It has also been reported that *TNF- $\alpha$* -stimulated neutrophils increase GPX4 expression during activation in ROS-dependent oxidative damage (Kanuri et al., 2011). NADPH oxidase (NOX), cyclooxygenase (COX) and LOX constantly generate free radicals such as ROS and NO, which, in addition to being used to kill pathogenic microorganisms, can activate NF- $\kappa$ B to induce the expression of proinflammatory cytokine genes in neighboring cells (Lu et al., 2017). In turn, NF- $\kappa$ B regulates the expression of COX-2 and 5-LOX (Hao et al., 2014), the proinflammatory cytokines *TNF- $\alpha$*  and *IL-1 $\beta$*  are stimulators of NOX, and ROS production triggers a positive feedback loop that contributes to the onset and persistence of inflammation (Liang et al., 2019).

It can be seen that the elevated iron content and the accumulation of ROS in spleen are likely due to changes in the expression of cytokines as well as ferroptosis-related genes, which in turn affect the expression of inflammatory cytokines and ferroptosis-related genes. Also, cytokines and ferroptosis-related genes interact with each other. These may all contribute to the development of ferroptosis under the action of LPS. Therefore, we used principal component analysis for further analysis. The results showed that component 2 had a large positive correlation with *TFR1*, iron, ROS, *IFN- $\gamma$* , and *TNF- $\alpha$* , and a larger negative correlation with T-AOC. This suggested that component 2 may mainly

represent iron overload leading to cellular lipid peroxidation and thus ferroptosis. The LPS group had the largest effect on component 2 and was positively correlated, which implied that LPS was an important influencing factor leading to ferroptosis in spleen of goslings. From the cluster of the 3D component plot, there was a positive correlation between cytokines and ferroptosis. In addition, we found a strong correlation between cytokines and antioxidant indicators. Moreover, the 4 principal component scores showed that the CON, PAMK, and LPS+PAMK groups had similar effects on the 4 components, with the LPS and PAMK groups showing the furthest difference in results. It indicates that PAMK treatment alleviated ferroptosis in spleen of goslings by LPS.

In conclusion, LPS not only causes inflammation and oxidative stress in the body, but also leads to ferroptosis through affecting the transcriptional regulation of ferroptosis-related genes. After treated with PAMK, the oxidative stress and increasing inflammatory cytokines caused by LPS could be alleviated, and together mitigate ferroptosis in spleen of goslings by regulating genes related to ferroptosis pathway.

## ACKNOWLEDGMENTS

This work was supported by National Natural Science Foundation of China (grant NO. 32102747), Guangdong Basic and Applied Basic Research Foundation (grant NO. 2019A1515110106), Natural Science Foundation of Hunan Province (grant NO. 2021JJ30312). The authors thank the members of the College of Animal Science & Technology, Guangdong Province Key Laboratory of Waterfowl Healthy Breeding for their help in collecting.

## DISCLOSURES

The authors declare no conflicts of interest.

## REFERENCES

- Armitage, A. E., L. A. Eddowes, U. Gileadi, S. Cole, N. Spottiswoode, T. A. Selvakumar, L. P. Ho, A. Townsend, and H. Drakesmith. 2011. Hepcidin regulation by innate immune and infectious stimuli. *Blood* 118:4129–4139.
- Bi, S., X. Ma, Y. Wang, X. Chi, and S. Hu. 2019. Protective effect of ginsenoside rg1 on oxidative damage induced by hydrogen peroxide in chicken splenic lymphocytes. *Oxidat. Med. Cell. Longevity* 2019:1–13.
- Chen, L., L. Peng, F. Xin, and C. Ma. 2017. Salidroside suppressing lps-induced myocardial injury by inhibiting ros-mediated pi3k/akt/mtor pathway in vitro and in vivo. *J. Cell. Mol. Med* 21:3178.
- Cheng, Z., and Y. Li. 2007. What is responsible for the initiating chemistry of iron-mediated lipid peroxidation: an update. *Chem. Rev.* 107:748–766.
- Dixon, S., K. Lemberg, M. Lamprecht, R. Skouta, E. Zaitsev, C. Gleason, D. Patel, A. Bauer, A. Cantley, and W. Yang. 2012. Ferroptosis: an iron-dependent form of nonapoptotic cell death. *Cell* 149:1060–1072.
- Farghali, H., K. M. Kgalalelo, L. Wojnarová, and C. Kutinová. 2015. In vitro and in vivo experimental hepatotoxic models in liver research: applications to the assessment of potential hepatoprotective drugs. *Physiol. Res.* 65:S417–S425.

- Gao, M., P. Monian, and X. Jiang. 2015. Metabolism and iron signaling in ferroptotic cell death. *Oncotarget* 6:35145–35146.
- Grenier, D., V. Goulet, and D. Mayrand. 2001. The capacity of porphyromonas gingivalis to multiply under iron-limiting conditions correlates with its pathogenicity in an animal model. *J. Dent. Res.* 80:1678–1682.
- Guo, S., W. Li, F. Chen, S. Yang, Y. Huang, Y. Tian, D. Xu, and N. Cao. 2021. Polysaccharide of atractylodes macrocephala koidz regulates lps-mediated mouse hepatitis through the tlr4-myd88-nfkb signaling pathway. *Int. Immunopharmacol.* 98:107692.
- Hao, Q., C. Zhang, Y. Gao, S. Wang, J. Li, M. Li, X. Xue, W. Li, W. Zhang, and Y. Zhang. 2014. Foxp3 inhibits nf- $\kappa$ b activity and hence cox2 expression in gastric cancer cells. *Cell. Signalling* 26:564–569.
- Hou, W., Y. Xie, X. Song, X. Sun, M. T. Lotze, H. J. Zeh, R. Kang, and D. Tang. 2016. Autophagy promotes ferroptosis by degradation of ferritin. *Autophagy* 12:1425–1428.
- Hua, H., X. Li, Y. Wang, X. Yang, S. Zhang, Y. Yang, Y. Liu, and X. Xu. 2019. Study on ferroptosis of jejunum epithelial cells in weaned piglets at different time after lipopolysaccharides challenge. *Chin. J. Anim. Husband* 055:78–82.
- Kain, H. S., E. Glennon, K. Vijayan, N. Arang, and A. Kaushansky. 2019. Liver stage malaria infection is controlled by host regulators of lipid peroxidation. *Cell Death Differ.* 27:1–11.
- Kanuri, G., A. Spruss, S. Wagnerberger, S. C. Bischoff, and I. Bergheim. 2011. Role of tumor necrosis factor  $\alpha$  (tnf $\alpha$ ) in the onset of fructose-induced nonalcoholic fatty liver disease in mice. *J. Nutr. Biochem.* 22:527–534.
- Karuppagounder, S., L. Alin, Y. Chen, D. Brand, M. Bourassa, K. Dietrich, C. Wilkinson, C. Nadeau, A. Kumar, S. Perry, J. Pinto, V. Darley-Usmar, S. Sanchez, G. Milne, D. Pratico, T. Holman, S. Carmichael, G. Coppola, F. Colbourne, and R. Ratan. 2018. N-acetylcysteine targets 5 lipoxygenase-derived, toxic lipids and can synergize with prostaglandin e to inhibit ferroptosis and improve outcomes following hemorrhagic stroke in mice. *Ann. Neurol.* 84:854–872.
- Kemna, E., P. Pickkers, E. Nemeth, H. Hoeven, and D. Swinkels. 2005. Time-course analysis of hepcidin, serum iron, and plasma cytokine levels in humans injected with lps. *Blood* 106:1864.
- Kroner, A., A. Greenhalgh, J. Zarruk, R. Passos dos Santos, M. Gaestel, and S. David. 2014. Tnf and increased intracellular iron alter macrophage polarization to a detrimental m1 phenotype in the injured spinal cord. *Neuron* 83:1098–1116.
- Li, N., W. Wang, H. Zhou, Q. Wu, M. Duan, C. Liu, H. Wu, W. Deng, D. Shen, and Q. Tang. 2020. Ferritinophagy-mediated ferroptosis is involved in sepsis-induced cardiac injury. *Free Radical Biol. Med.* 160:303–318.
- Li, N., H. Zhou, H. Wu, Q. Wu, and Q. Tang. 2019a. Sting-irf3 contributes to lipopolysaccharide-induced cardiac dysfunction, inflammation, apoptosis and pyroptosis by activating nlrp3. *Redox. Biol.* 24:101215.
- Li, W., N. Cao, Y. Tian, X. Xiang, B. Li, Y. Huang, and D. Xu. 2019b. Polysaccharide of atractylodes macrocephala koidz regulates goslins spleen lymphocyte immune function through tlr4/nfkb signaling pathway. *Chin. J. Anim. Nutr.* 31:299–308.
- Li, W., G. Feng, J. M. Gauthier, I. Lokshina, and D. Kreisel. 2019c. Ferroptotic cell death and tlr4/trif signaling initiate neutrophil recruitment after heart transplantation. *J. Clin. Invest.* 130:2293–2304.
- Li, W., S. Guo, D. Xu, B. Li, N. Cao, Y. Tian, and Q. Jiang. 2018. Polysaccharide of atractylodes macrocephala koidz (pamk) relieves immunosuppression in cyclophosphamide-treated geese by maintaining a humoral and cellular immune balance. *Molecules* 23:932.
- Li, W., X. Xiang, N. Cao, W. Chen, Y. Tian, X. Zhang, X. Shen, D. Jiang, D. Xu, and S. Xu. 2021a. Polysaccharide of atractylodes macrocephala koidz activated t lymphocytes to alleviate cyclophosphamide-induced immunosuppression of geese through novel\_mir2/cd28/ap-1 signal pathway. *Poult. Sci.* 100:101129.
- Li, W., X. Xiang, B. Li, Y. Wang, and N. Cao. 2021b. Pamk relieves lps-induced enteritis and improves intestinal flora disorder in goslins. *Evid. Based Complement. Alternat. Med.* 2021:1–16.
- Li, X., F. Liu, Z. Li, N. Ye, C. Huang, and X. Yuan. 2014. Atractylodes macrocephala polysaccharides induces mitochondrial-mediated apoptosis in glioma c6 cells. *Int. J. Biol. Macromol.* 66:108–112.
- Liang, S., H. Y. Ma, Z. Zhong, D. Dhar, X. Liu, J. Xu, Y. Koyama, T. Nishio, D. Karin, and G. Karin. 2019. NADPH oxidase 1 in liver macrophages promotes inflammation and tumor development in mice - sciencedirect. *Gastroenterology* 156:1156–1172.
- Liu, P., Y. Feng, H. Li, X. Chen, G. Wang, S. Xu, Y. Li, and L. Zhao. 2020. Ferrostatin-1 alleviates lipopolysaccharide-induced acute lung injury via inhibiting ferroptosis. *Cell. Mol. Biol. Lett.* 25:10.
- Lu, W., J. Kang, K. Hu, S. Tang, X. Zhou, L. Xu, Y. Li, and S. Yu. 2017. The role of the nox4-derived ros-mediated rhoa/rho kinase pathway in rat hypertension induced by chronic intermittent hypoxia. *Sleep Breath* 21:667–677.
- Ludwiczek, S., E. Aigner, I. Theurl, and G. Weiss. 2003. Cytokine-mediated regulation of iron transport in human monocytic cells. *Blood* 101:4148–4154.
- Luo, H., and R. Zhang. 2021. Icarin enhances cell survival in lipopolysaccharide-induced synoviocytes by suppressing ferroptosis via the xc-/gpx4 axis. *Exp. Ther. Med.* 21:72.
- Maloberti, P. M., A. B. Duarte, U. D. Orlando, M. E. Pasqualini, Á. Solano, L. O. Carlos, E. Podestá, and S. Janine. 2010. Functional interaction between acyl-coa synthetase 4, lipoxygenases and cyclooxygenase-2 in the aggressive phenotype of breast cancer cells. *PLoS One* 5:e15540.
- Matsushita, M., S. Freigang, C. Schneider, M. Conrad, G. Bornkamm, and M. Kopf. 2015. T cell lipid peroxidation induces ferroptosis and prevents immunity to infection. *J. Exp. Med.* 212:1–14.
- Mishima, E., E. Sato, J. Ito, K. Yamada, C. Suzuki, Y. Oikawa, T. Matsushashi, K. Kikuchi, T. Toyohara, T. Suzuki, S. Ito, K. Nakagawa, and T. Abe. 2020. Drugs repurposed as ferroptosis agents suppress organ damage, including aki, by functioning as lipid peroxyl radical scavengers. *J. Am. Soc. Nephrol.* 31:280–296.
- Muckenthaler, M. U., S. Rivella, M. W. Hentze, and B. Galy. 2017. A red carpet for iron metabolism. *Cell* 168:344–361.
- Nemeth, E., S. Rivera, V. Gabayan, C. Keller, and T. Ganz. 2004. Il-6 mediates hypoferrremia of inflammation by inducing the synthesis of the iron regulatory hormone hepcidin. *J. Clin. Invest.* 113:1271.
- Nicolas, G. 2002. The gene encoding the iron regulatory peptide hepcidin is regulated by anemia, hypoxia, and inflammation. *J. Clin. Invest.* 110:1037–1044.
- Proneth, B., and M. Conrad. 2019. Ferroptosis and neuroinflammation, a yet poorly explored link. *Cell Death Differ.* 26:14–24.
- Qiang, Yu, Shao-Ping, Nie, Jun-Qiao, Wang, Peng-Fei, Yin, Dan-Fei and Huang (2014) Toll-like receptor 4-mediated  $\{\text{ros}\}$  signaling pathway involved in ganoderma atrum polysaccharide-induced tumor necrosis factor- $\alpha$  secretion during macrophage activation. *Food Chem. Toxicol.*
- Reuter, S., S. C. Gupta, M. M. Chaturvedi, and B. B. Aggarwal. 2010. Oxidative stress, inflammation, and cancer: how are they linked? *Free Radical Biol. Med.* 49:1603–1616.
- Shu, Y., K. Kao, and C. Weng. 2017. In vitro antibacterial and cytotoxic activities of plasma-modified polyethylene terephthalate non-woven dressing with aqueous extract of rhizome atractylodes macrocephala. *Mat. Sci. Eng. C Mat. Biol. Appl.* 77:606–612.
- Wang, J., J. Chen, and K. Pan. 2013. Effect of exogenous abscisic acid on the level of antioxidants in atractylodes macrocephala koidz under lead stress. *Environ. Sci. Pollut. Res. Int.* 20:1441–1449.
- Wang, L., L. Harrington, E. Trebicka, H. N. Shi, J. C. Kagan, C. C. Hong, H. Y. Lin, J. L. Babitt, and B. J. Cherayil. 2009. Selective modulation of tlr4-activated inflammatory responses by altered iron homeostasis in mice. *J. Clin. Invest.* 119:3322–3328.
- Xiang, X., N. Cao, F. Chen, L. Qian, Y. Wang, Y. Huang, Y. Tian, D. Xu, and W. Li. 2020. Atractylodes macrocephalapolysaccharide of koidz (pamk) alleviates cyclophosphamide-induced immunosuppression in mice by upregulating cd28/ip3r/plc $\gamma$ -1/ap-1/nfat signal pathway. *Front. Pharmacol.* 11:529657.
- Xiao, K., W. H. Zou, Z. Yang, Z. U. Rehman, A. R. Ansari, H. R. Yuan, Y. Zhou, L. Cui, K. M. Peng, and H. Song. 2015. The role of visfatin on the regulation of inflammation and apoptosis in the spleen of lps-treated rats. *Cell Tissue Res.* 359:605–618.

- Xie, Y., W. Hou, X. Song, Y. Yu, J. Huang, X. Sun, R. Kang, and D. Tang. 2016. Ferroptosis: process and function. *Cell Death Different.* 23:369–379.
- Xiong, S., H. She, H. Takeuchi, B. Han, J. F. Engelhardt, C. Barton, E. Zandi, C. Giulivi, and H. Tsukamoto. 2003. Signaling role of intracellular iron in  $\text{nf-}\kappa\text{b}$  activation. *J. Biol. Chem.* 278:17646–17654.
- Xu, D., B. Li, N. Cao, W. Li, Y. Tian, and Y. Huang. 2017. Atractyodes macrocephalathe protective effects of polysaccharide of koidz (pamk) on the chicken spleen under heat stress via antagonizing apoptosis and restoring the immune function. *Oncotarget* 8:70394–70405.
- Yang, W., R. Sriramaratnam, M. Welsch, K. Shimada, R. Skouta, V. Viswanathan, J. Cheah, P. Clemons, A. Shamji, and C. Clish. 2014. Regulation of ferroptotic cancer cell death by  $\text{gpx4}$ . *Cell* 156:317–331.
- Zhang, Z., Z. Fan, P. An, X. Guo, and F. Wang. 2011. Ferroportin1 deficiency in mouse macrophages impairs iron homeostasis and inflammatory responses. *Blood* 118:1912–1922.
- Zhao, Y., J. Li, W. Guo, H. Li, and L. Lei. 2020. Periodontitis-level butyrate-induced ferroptosis in periodontal ligament fibroblasts by activation of ferritinophagy. *Cell Death Discov.* 6:119.